JOURNAL OF APPLIED ELECTROCHEMISTRY 21 (1991) 659–666

Reticulated vitreous carbon cathodes for metal ion removal from process streams
Part I: Mass transport studies

D. PLETCHER, I. WHYTE
Department of Chemistry, The University, Southampton SO9 5NH, Great Britain

F. C. WALSH
Chemistry Department, Portsmouth Polytechnic, Portsmouth PO1 2DT, Great Britain

J. P. MILLINGTON
Electricity Research and Development Centre, Capenhurst, Chester CH1 6ES, Great Britain

Received 31 October 1990; revised 12 February 1991

The cathodic deposition of copper from acid sulphate solution containing copper(II) has been used to characterize the mass transport properties of reticulated vitreous carbon cathodes, operated in the flow-by mode. Current-potential curves recorded at a rotating vitreous carbon disc electrode were used to determine the diffusion coefficient for copper(II) under the conditions of the experiments and also to elucidate the effect of oxygen in the electrolyte stream. Pressure drop measurements have been used to separate the mass transport coefficient and real surface area effect for four grades of reticulated vitreous carbon, nominally having 10, 30, 60, 100 pores per inch.

1. Introduction

The fifteen year period up to 1980 saw a substantial growth of electrochemical engineering as an academic discipline. One objective was the development of three-dimensional electrode technology for the removal of metal ions from effluents. Indeed, these efforts led to the appearance on the market of several technologies including the Chemelec cell [1, 2], the EnviroCell [3, 4], the Retec Cell [5, 6] and the ElectroSyn and ElectroProd cells containing packed bed electrodes [7, 8]. The performance of such cells and the literature from the period have both been extensively reviewed, for example [9–17]. In terms of the conversion efficiency, most of these systems are, however, known to operate most satisfactorily when the metal ion concentration is significantly greater than 10 p.p.m. On the other hand, maximum metal ion levels permitted in discharges are commonly below 1 p.p.m. Hence, one purpose of our programme is to reassess three-dimensional electrode technology and to determine whether it can operate economically to very low metal ion levels. It is also intended to carry out parallel, fundamental studies in order to understand more quantitatively the metal removal technology, including the additional problems found in practice which result from the presence of dissolved oxygen, complexing agents and mixtures of metal ions as well as pH changes at the cathode surface.

In this first paper of the series, the reduction of copper(II) in acid sulphate solution is used to characterize mass transport to four grades of reticulated vitreous carbon (10, 30, 60 and 100 pores per inch). These materials were selected because of their regular structure, high area/volume ratio, high porosity and good electrical conductivity (*cf.* other three-dimensional electrodes). The properties and electrochemical applications of reticulated vitreous carbon have been reviewed [18]. Reticulated vitreous electrodes have been used in analytical chemistry [19–23] and also for the removal of metal ions from solution [24–26]. There are also earlier studies of the related, metal foam electrodes [27, 28] and a recent series of papers has reported a detailed investigation of mass transport to nickel foams [29–32]. The Retec cell [5, 6] is, of course, based on reticulated electrodes (Cu, Ni or C).

2. Experimental details

The flow cell is sketched in Fig. 1. The cell was machined from four blocks of polypropylene (each 280 mm × 100 mm and 12 mm thick). The lead anode (50 × 50 mm) and the steel plate cathodic current collector (also 50 mm × 50 mm) were mounted into the outer polypropylene blocks so that their surfaces were flush with the surface of the polymer. The inner polypropylene blocks formed the electrolyte channels; these were shaped to give extended entry and exit lengths while the reticulated carbon cathode (50 mm × 50 mm × 12 mm) fitted tightly into the centre of the catholyte channel; electrical contact to the stainless steel current collector was made with a conducting

© 1991 Chapman and Hall Ltd.

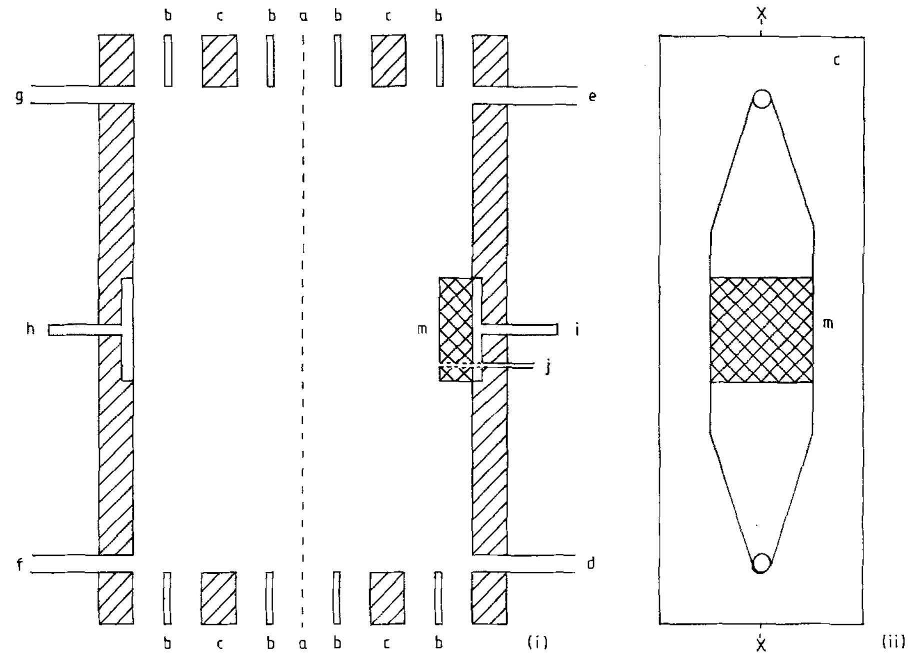

Fig. 1. (i) Expanded view of cell showing: (a) Nafion 417 membrane, (b) silicone "Viton" gaskets, (c) polypropylene blocks with flow channels, (d) catholyte inlet, (e) catholyte outlet, (f) anolyte inlet, (g) anolyte outlet, (h) Pb anode (i) steel cathode feeder, (j) reference electrode port, and (m) reticulated vitreous carbon electrode. (ii) Plan view of catholyte channel across X-X including reticulated vitreous carbon cathode.

carbon cement (Leit-C from Agar Aids). The four grades of reticulated vitreous carbon (10, 30, 60 and 100 pores per inch) were manufactured by Energy Research and Generation Inc. and supplied by The Electrosynthesis Co Inc. The anolyte and catholyte compartments were separated by a Nafion® 417 cation permeable membrane (Dupont). This membrane allowed proton transport from anolyte to catholyte and was preferred to an anion permeable membrane because of its higher chemical stability. 1 mm silicone rubber gaskets were placed between each of the cell components to prevent electrolyte leakage. After compression, the reticulated vitreous carbon was a close fit in the channel; flow visualization experiments showed that no significant bulk bypassing by the electrolyte occurred. The cell had two electrolyte entry and two electrolyte exit ports wth 0.5 inch 'Fast and Tite' fittings. A Luggin capillary entered the catholyte compartment through a 3 mm hole bored through the cathode contact plate. The reference electrode was always a Radiometer type K401 saturated calomel electrode.

The hydraulic circuit is shown schematically in Fig. 2. The anolyte and catholyte reservoirs were each filled with 3 dm^3 of electrolyte. The electrolytes were circulated using two Totton EMP 40/4 pumps. The catholyte flow was controlled with a KDG 18XE flowmeter which gave a range from 0 to 8 $dm^3 min^{-1}$ and hence a mean linear flow velocity range of 0 to 0.22 $m s^{-1}$ in the cell described above. The catholyte reservoir was fitted with a nitrogen sparger to aid the removal of dissolved oxygen. With the exception of the glass reservoirs, the electrolyte circuits were constructed only from PVC pipework, GF 0.5 inch valves and Gielle 3-way connectors.

The electrolytes were prepared with Millipore water and Analar reagents. The anolyte was always 0.5 mol dm^{-3} sodium sulphate adjusted to pH 2 by the addition of sulphuric acid. Except where otherwise stated, the catholyte was 0.5 mol dm^{-3} sodium sulphate, pH 2, containing the specified concentration of copper sulphate.

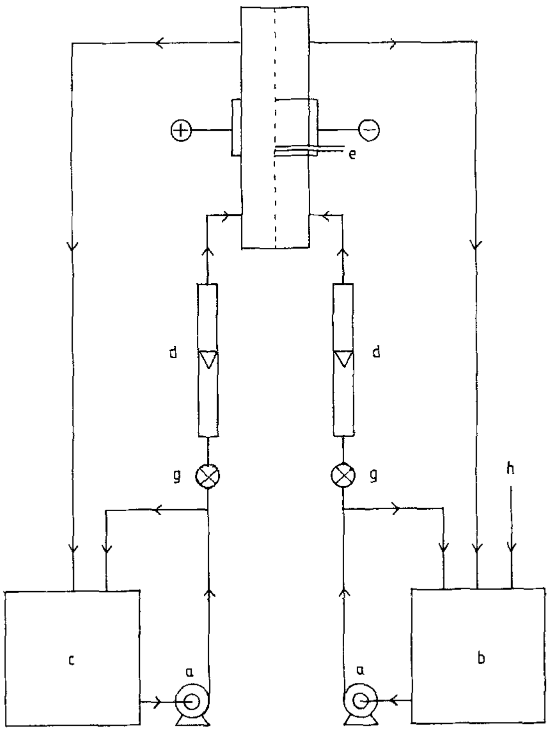

Fig. 2. Hydraulic flow circuit showing: (a) pumps, (b) catholyte reservoir, (c) anolyte reservoir, (d) flowmeters, (e) reference electrode position, (g) valves and (h) nitrogen sparger.

Experiments with the rotating vitreous carbon disc electrode (area $12.5 \times 10^{-6}\,\mathrm{m}^2$) were carried out in a small, three compartment, glass cell. The disc and Pt gauze counter electrodes were separated by a glass frit and the SCE reference electrode was mounted within a Luggin capillary. All experiments were carried out at $298 \pm 1\,\mathrm{K}$.

All electrochemical experiments were controlled with a HiTek potentiostat, type DT2101, and function generator, type PPR1, while the response was recorded on a Gould 60000 xy recorder. Electrical charge was measured using a home built digital integrator. The analyses for copper(II) were carried out by atomic absorption spectroscopy using an Instrumentation Lab., model 157, with an oxygen/acetylene flame. The unknowns were found by comparison of the response with a linear calibration plot obtained with standards 0, 1, 2 and 4 p.p.m. prepared from a Spectrosol AA standard solution (BDH Ltd).

3. Definitions and theory

When the conditions are chosen so that the reduction of copper(II) to copper metal is mass transport controlled over all the surface of the three-dimensional cathode, the current is given by

$$I_L = 2FV_e k_m A_e c \qquad (1)$$

where V_e is the volume of the cathode, A_e is the specific surface area (the active area/unit volume of cathode) and k_m is the mass transfer coefficient and c is the concentration of copper(II). Hence, Equation 1 may be used to calculate $k_m A_e$ from the cell current provided (a) the cathode potential is chosen so that the reduction of copper(II) is mass transport controlled but no other reaction occurs, (b) the potential distribution is sufficiently uniform through the cathode and (c) the depletion of the copper(II) in solution during a single pass through the cathode is insignificant (in the worst situation the depletion is 18%).

The quantity $k_m A_e$ was also estimated by following the concentration of copper(II), $c(t)$, as a function of time during controlled potential electrolysis. It may be shown [33] that the present system may be modelled very satisfactorily as a simple batch reactor and there is no significant need to use a batch-recycle model. For a batch system

$$c(t) = c(0)\exp\left[-V_e k_m A_e t/V_R\right] \qquad (2)$$

or

$$\ln\left[c(t)/c(0)\right] = -V_e k_m A_e t/V_R \qquad (3)$$

where V_R is the total volume of catholyte.

The specific surface areas, A_e, were estimated from measurements of the static pressure drop/unit height of the three-dimensional, porous structure, $\Delta P/H$, as a function of the linear flow velocity, v, using the Ergun equation [30, 34, 35]

$$\Delta P/H = Mv^2 + Nv \qquad (4)$$

and A_s, the specific surface area/unit of solid volume, may be calculated from the intercept and slope via the relationship

$$A_s^4 = \frac{N^3(0.096H\rho)^2}{M^2(5\gamma\mu H)^3}\,\frac{\varepsilon^3}{(1-\varepsilon)^4} \qquad (5)$$

where ρ is the electrolyte density and μ its dynamic viscosity. γ is known as the circularity factor of the pores and its value is commonly taken as 1.25; the value of A_s is not sensitive to reasonable choices of this parameter. ε is the mean porosity for which the manufacturers give the approximate value 0.97 for the reticulated vitreous carbons. It should also be noted that in [30], an error exists in the published version of Equation 5; the five in the denominator is unfortunately given as a two. A_e and A_s are related by the equation

$$A_e = A_s(1-\varepsilon) \qquad (6)$$

Mass transport data were correlated using the dimensionless relationship

$$Sh = a\,Re^b Sc^{0.33} \qquad (7)$$

where the Sherwood and Reynolds numbers are defined by

$$Sh = k_m d_e/D \qquad (8)$$

$$Re = v d_e \rho/\mu \qquad (9)$$

and Sc is the Schmidt number. The characteristic length, d_e, was based on the channel dimensions, the hydraulic diameter being used.

$$d_e = 2BS/(B+S) \qquad (10)$$

where B and S are the width and thickness of the channel (they are also the dimensions of the reticulated carbon cathode).

4. Results and discussion

4.1. *Rotating disc electrode experiments*

Figure 3 shows a set of *I–E* curves recorded using a potential scan rate of $10\,\mathrm{mV\,s^{-1}}$ for a vitreous carbon disc electrode. Rotation rates 400–3600 r.p.m., in a deaerated solution containing $1\,\mathrm{mmol\,dm^{-3}}$ (64 p.p.m.) copper(II) in $0.5\,\mathrm{mol\,dm^{-3}}$ sodium sulphate, pH 2. It can be seen that a simple, well-formed reduction wave is observed with $E_{1/2} = -240\,\mathrm{mV/SCE}$. Moreover, a plot of I_L against $\omega^{1/2}$ is linear confirming that the copper deposition becomes mass transport controlled; using a value of $1.17 \times 10^{-6}\,\mathrm{m^2\,s^{-1}}$ for the kinematic viscosity of the electrolyte [36], the diffusion coefficient was calculated to be $4.9 \times 10^{-10}\,\mathrm{m^2\,s^{-1}}$ [37]. Figure 4 shows a similar set of curves after the same solution had been air sparged for approximately 30 min. The wave for oxygen reduction is observed at $E_{1/2} = -570\,\mathrm{mV/SCE}$. Although there is always a short limiting current plateau for copper(II) reduction, particularly at low rotation rates, there is some overlap of the two reduction waves and the limiting currents for $1\,\mathrm{mmol\,dm^{-3}}$ copper(II) and the concentration of

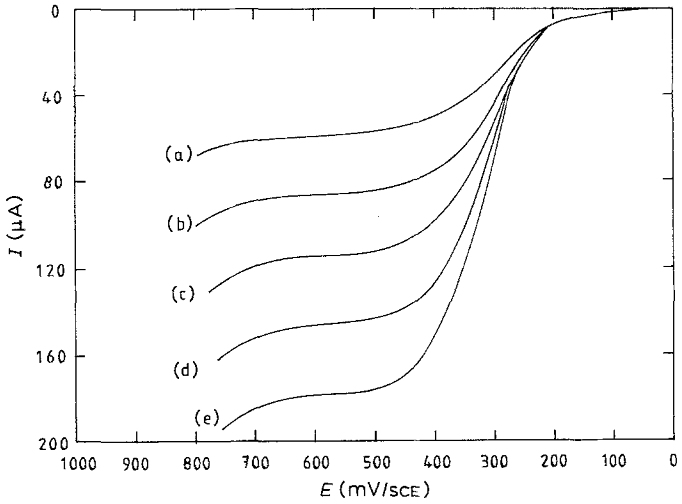

Fig. 3. Current-potential curves for the reduction of 1 mmol dm^{-3} copper(II) in a nitrogen purged 0.5 mol dm^{-3} sodium sulphate, pH 2 solution at a rotating vitreous carbon disc electrode (A = 1.25 × 10^{-5}m^2), for rotation rates of: (a) 400, (b) 900, (c) 1600, (d) 2500 and (e) 3600 rev. min^{-1}. Potential sweep rate 10 mV s^{-1}. T = 297 K.

oxygen resulting from equilibration with air are similar. Clearly, as the concentration of copper(II) is decreased, interference from oxygen in the medium must become more pronounced and it will become more difficult to define a potential where one can obtain a high rate of copper(II) reduction without also reducing oxygen. Rotating disc experiments were also carried out with 0.1 mmol dm^{-3} (6.4 p.p.m.) and 10 mmol dm^{-3} (635 p.p.m.) copper(II) in the same medium. In both cases, it was possible to obtain well-defined reduction waves and the rotation rate dependence was used to estimate values for the diffusion coefficient of copper(II), see Table 1. In the case of the lowest copper(II) concentration, however, it was very difficult to remove all the oxygen and hence its reduction wave could always be seen. The limiting current for copper(II) reduction was estimated as the current measured at −0.50 V.

Table 1 reports the diffusion coefficients for copper(II) determined in this study and also some values taken from the literature for similar sulphate media at 298 K. It appears that the values in sodium sulphate solution are slightly lower than those in sulphuric acid.

4.2. *Current-potential data with reticulated carbon electrodes*

Figure 5 shows a set of I–E curves recorded using a potential scan rate of 5 mV s^{-1} for a 1 mmol dm^{-3} (64 p.p.m.) copper(II) solution in 0.5 mol dm^{-3} sodium sulphate, pH 2, for various flow rates through 10 p.p.i. reticulated carbon. Reasonable reduction waves are observed, $E_{1/2} \approx -310$ mV. The limiting current increases with flow rate although, particularly at higher flow rates, the plateaux show an appreciable slope. Similar data are obtained with the other three grades of reticulated carbon and it was also confirmed that the limiting currents were proportional to the copper(II) concentration. The limiting currents are, as expected, much higher on the reticulated materials than with a flat plate cathode; for example, with the 100 p.p.i. reticulated carbon, the current is some 250 times larger than with the stainless steel cathode contact plate alone. Equation 1 was used to calculate $k_m A_e$ from the limiting currents, either measured directly from the I–E curves at −500 mV or following a potential step experiment from 0 mV to −500 mV (the "steady state" current was measured after 90 s –

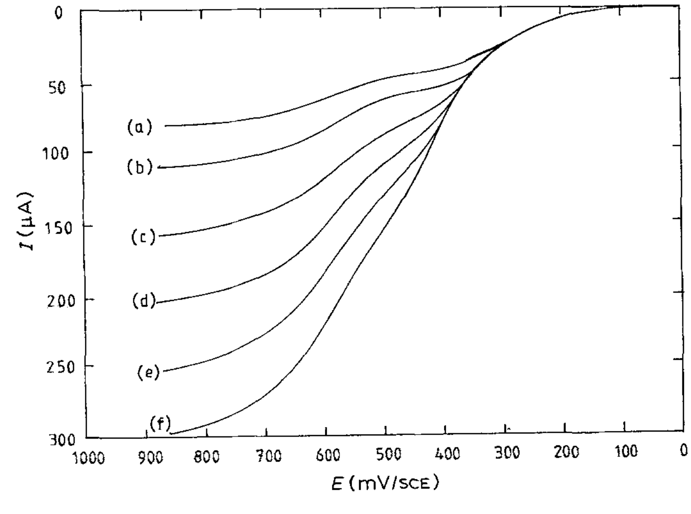

Fig. 4. Current-potential curves for the reduction of 1 mmol dm^{-3} copper(II) in an air saturated 0.5 mol dm^{-3} sodium sulphate, pH 2 solution at a rotating vitreous carbon disc electrode (A = 1.25 × 10^{-5}m^2), for rotation rates of: (a) 200, (b) 400, (c) 900, (d) 1600, (e) 2500 and (f) 3600 rev. min^{-1}. Potential sweep rate 10 mV s^{-1}. T = 298 K.

Table 1. Diffusion coefficients for copper(II) in aqueous sulphate media at 298 K.

$[Cu^{2+}]$ (mmol dm^{-3})	*Medium*	$10^{10}D$ ($m^2 s^{-1}$)	*Reference*
10	0.5 mol dm^{-3} Na_2SO_4, pH 2	4.9	this work
1		4.8	this work
0.1		4.8	this work
11	0.7 mol dm^{-3} H_2SO_4	5.8	[38]
40	0.5 mol dm^{-3} H_2SO_4	6.0	[39]

Table 2. Specific surface areas estimated from pressure drop measurements and use of the Ergun equation.

*Grade (p.p.i.)**	A_e (m^{-1})
10	1300 ± 900
30	2400 ± 900
60	3200 ± 1000
100	6700 ± 250

* nominal pores per inch.

the transient response also showed the effects of nucleation of the metal phase on the carbon surface). Plots of $k_m A_e$ as a function of the mean linear flow rate are shown in Fig. 6. It can be seen that the values of $k_m A_e$ vary significantly with the grade of reticulated carbon. They are, however, of the same magnitude to those reported by Langlois and Coeuret [31] for ferricyanide reduction at nickel foams. A quantitative comparison of $k_m A_e$ values between the RVC and other cathode materials will be presented elsewhere [40].

4.3. *Controlled potential electrolyses at reticulated carbon cathodes*

The quantity can also be determined by monitoring the depletion of copper(II) during controlled potential electrolyses at potentials where the reduction is mass transfer controlled, see Equations 2 and 3. Figure 7 shows the results of such experiments as a plot of log $[c(t)/c(0)]$ against t. In each case, the electrolysis was carried out at −500 mV (chosen to minimize the interference from oxygen reduction (see § 4.1)) with an initial Cu(II) concentration of approximately 10 p.p.m. and a linear flow rate of 0.083 m s^{-1}. For an order of magnitude decrease in the copper(II) concentration, the semilog plot is linear corresponding to a first order decay, see Equation 3. This was also the case for a series of electrolyses carried out at as a function of flow rate, see Fig. 8. The values of $k_m A_e$ from these experiments are also shown on Fig. 6 and it is clear that there is good agreement with the data from measurements of the limiting current.

4.4. *Estimation of A_e from pressure drop measurements*

For this series of experiments, the pressure at the base and the top of the reticulated carbon cathodes was measured via capillaries through the catholyte block and attached to water manometers. Figure 9 reports the pressure drop as a function of the mean linear flow rate for the four grades of reticulated carbon; the plots are linear as predicted by Equation 4 and the slopes and intercepts were used to estimate values of A_e, see Table 2, for the four grades of reticulated vitreous carbon. The errors in this procedure are large because of the rather small pressure drops, particularly with the 10 and 30 p.p.i. samples, and also because of the uncertainties associated with the estimation. The values determined are, however, in agreement with previous estimates for reticulated vitreous carbon and other foams as may be seen from a comparison table drawn up by Langlois and Coeuret [30].

5. Conclusions

The values of A_e may be used to separate the area and mass transport factors contributing to the enhanced limiting current at the three-dimensional materials and hence to convert the data of Fig. 6 to a dimensionless plot of Sherwood against Reynolds numbers (for definitions, see § 3). Figure 10 shows such plots

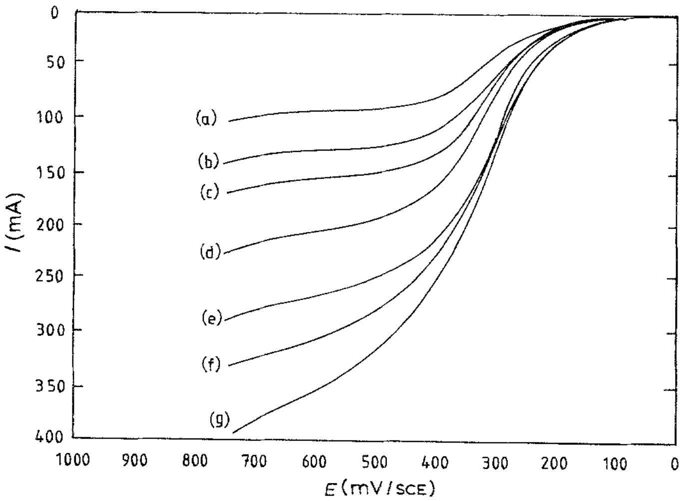

Fig. 5. Current-potential curves for the reduction of 1 mmol dm^{-3} copper(II) in a nitrogen purged 0.5 mol dm^{-3} sodium sulphate, pH 2 solution at a 10 p.p.i. reticulated vitreous carbon foam. Mean linear flow rates: (a) 0.023, (b) 0.034, (c) 0.050, (d) 0.083, (e) 0.128, (f) 0.151 and (g) 0.208 m s^{-1}. Potential sweep rate 5 mV s^{-1}. T = 298 K.

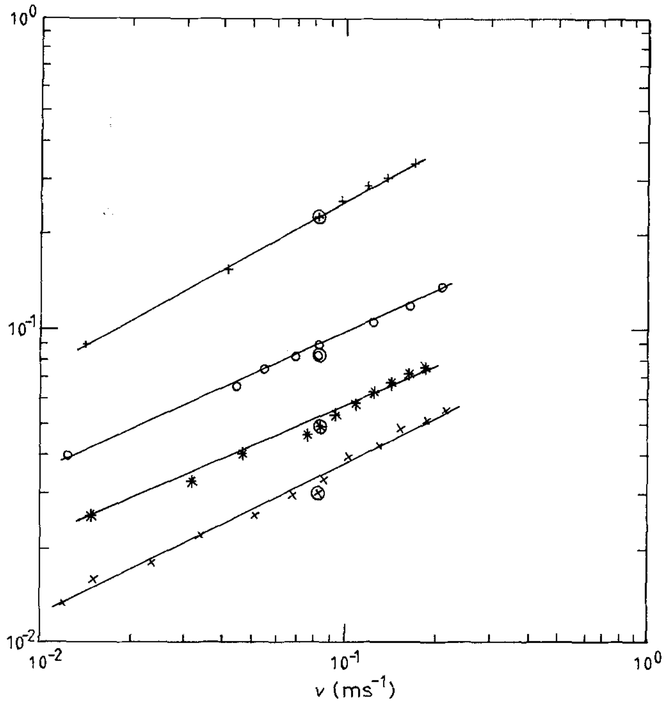

Fig. 6. Variation of $k_m A_e$ with mean linear flow rate for four grades of reticulated vitreous carbon in 0.5 mol dm^{-3} Na_2SO_4, pH 2. (x) Data for 10 p.p.i. calculated from the current at -500 mV during a potential sweep at 5 mV s^{-1}. (∗) Data for 30 p.p.i. (as 10 p.p.i.). (O) Data for 60 p.p.i. calculated from the current 90 s after a potential step to -500 mV. (+) Data for 100 p.p.i. (as 60 p.p.i.). The circled points show the $k_m A_e$ values for the four grades of reticulated vitreous carbon calculated from the controlled potential electrolysis (see Fig. 7).

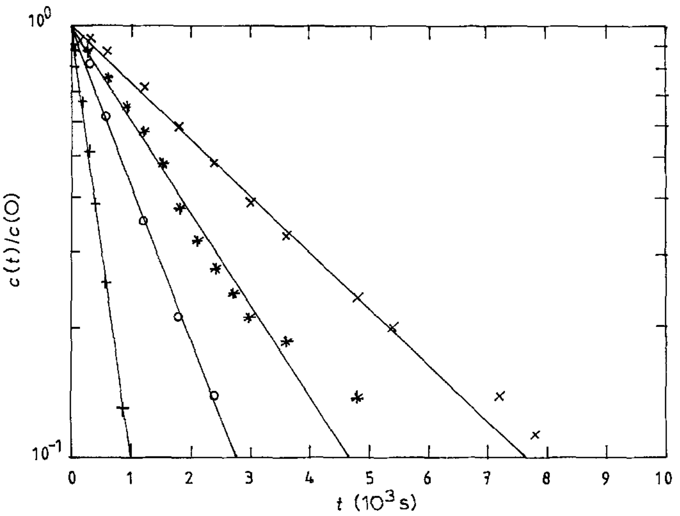

Fig. 7. Logarithm of normalized copper concentration against time for 10 (x), 30 (∗), 60 (O) and 100 (+) p.p.i. reticulated vitreous carbon. Controlled potential electrolysis at -500 mV/SCE. $c(0) = 0.16$ mmol dm^{-3} (10 p.p.m.) Cu^{2+} in a nitrogen purged 0.5 mol dm^{-3} sodium sulphate, pH 2 solution. $v = 0.083$ m s^{-1}. $T = 299$ K.

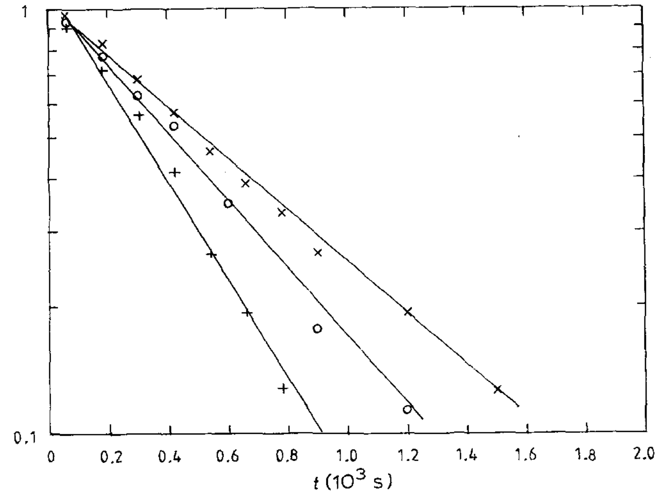

Fig. 8. Logarithm of normalized copper concentration against time curves for a 0.03 mmol dm^{-3} (2 p.p.m.) Cu^{2+} in a nitrogen purged 0.5 mol dm^{-3} sodium sulphate, pH 2 solution at a 100 p.p.i. reticulated vitreous carbon foam. Mean linear flow rates of 0.042 (x), 0.083 (O) and 0.125 (+) m s^{-1}. Potential -500 mV/SCE. $T = 298$ K.

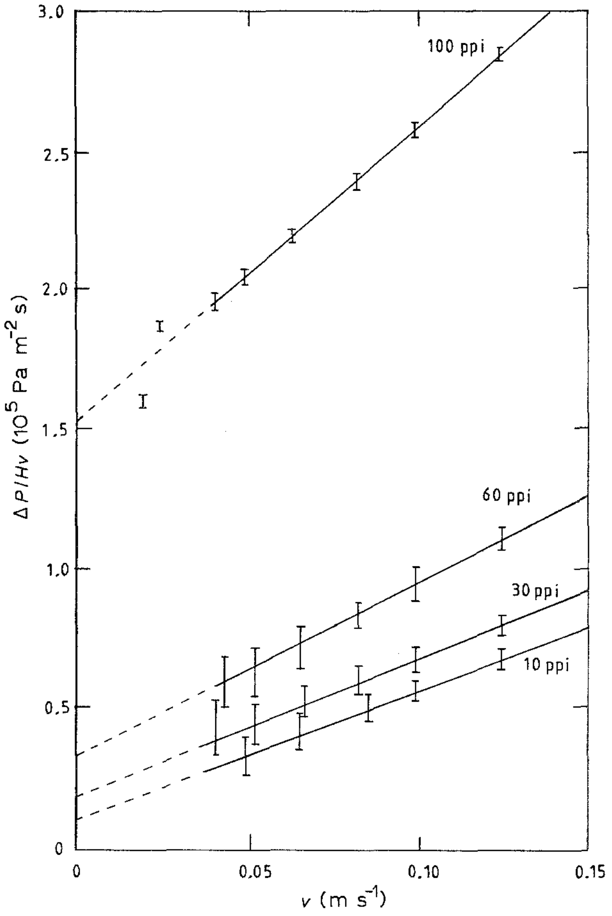

Fig. 9. $\Delta P/Hv$ against v according to the Ergun equation (Equation 4) for the four grades of reticulated vitreous carbon.

for both the four reticulated carbons and also for a flat plate cathode in the same cell. The data for the flat plate cathode shows the change of slope previously reported in the literature for such electrodes, for example see Lapique *et al.* [41]. The figure clearly demonstrates the following:

(a) The large enhancement in the limiting current densities at the reticulated carbons ($\sim$ 100–250 compared to a flat plate) primarily results from their very high surface areas.

(b) There is also a contribution from turbulence introduced by the porous structure but it is small and certainly no more than a factor of two.

(c) Within the errors introduced by the experimental techniques used, particularly the pressure drop measurements, it is not possible to demonstrate significant differences in the mass transport properties of the four grades of reticulated vitreous carbon. Hence, the data for all four materials has been fitted to a single, approximate correlation equation.

$$Sh = 2.7\,(Re)^{0.48}(Sc)^{0.33} \tag{11}$$

It is not possible to compare this Sherwood-Reynolds correlation with that reported by Langlois and Coeuret [31]; these authors, perhaps more correctly from a theoretical viewpoint, chose to base the Reynolds number on the dimensions of the pore in the three dimensional cathode material. We have preferred to use a characteristic dimension associated with the flow channel dimensions; this allows direct comparison with other electrode geometries in the same cell.

In part II of this series, the performance of the reticulated carbon materials for the removal of copper ions from acid sulphate is discussed and it is shown that copper ion levels may be reduced below 0.1 p.p.m. with good efficiency.

References

[1] C. L. Lopez-Cacicedo, *J. Separ. Proc. Technol.* **2** (1981) 34.
[2] Marketed by BEWT (Water Engineers) Ltd, Tything Road, Arden Forest Industrial Estate, Alcester, Warwickshire, England.
[3] G. Kreysa and C. Reynvaan, *J. Appl. Electrochem.* **12** (1982) 241.
[4] Marketed by Deutsche Carbone Akt., Post 560209, Talstrasse 112, 6000 Frankfurt/Main, West Germany.
[5] M. G. Konicek and G. Platek, *New Materials and New Processes* **2** (1983) 232.

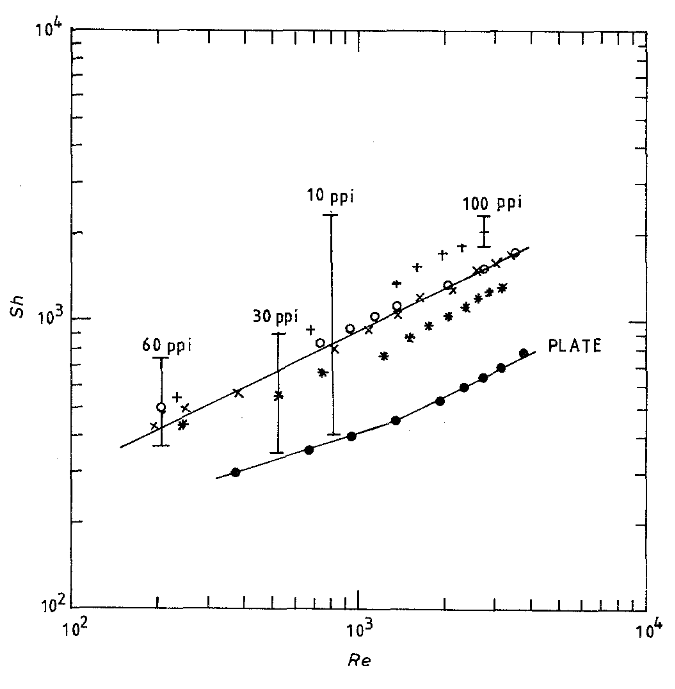

Fig. 10. Sherwood-Reynolds correlations for a flat plate, 10 (x), 30 (*), 60 (O) and 100 (+) p.p.i. reticulated vitreous carbon foams. The error bars indicate the typical errors for each grade of reticulated carbon. The solid line corresponds to Equation 11.

[6] Marketed by EES Corporation, 12850 Bournewood Drive, Sugar Land, TX 77478, USA.

[7] D. Simonsson, *J. Appl. Electrochem.* **14** (1984) 595.

[8] Marketed by ElectroCell AB, Tumstockvagen 10, S-18366 Taby, Sweden.

[9] D. Pletcher and F. C. Walsh, 'Industrial Electrochemistry', Chapman and Hall, London (1990).

[10] 'Electrochemical Reactors – Their Science and Technology, Part A' (edited by M. I. Ismail) Elsevier, Amsterdam (1989).

[11] R. J. Marshall and F. C. Walsh, *Surface Technol.* **24** (1985) 45.

[12] B. Fleet, *Coll. Czech. Chem. Comm.* **53** (1988) 1107.

[13] J. L. Weininger, *AIChE Symp. Series*, No 229, **79** (1983) 179.

[14] G. Kreysa, *Metalloberflache* **35** (1981) 6.

[15] J. S. Newman and W. Tiedeman, *Adv. Electrochem. and Electrochem. Engng* **11** (1978) 353.

[16] R. E. Sioda and K. B. Keating, *Electroanal. Chem.* **12** (1982) 1.

[17] D. Pletcher, F. C. Walsh and I. Whyte, *I. Chem. E. Symp. Series* **116** (1990) 195.

[18] J. Wang, *Electrochim. Acta* **26** (1981) 1721.

[19] A. N. Strohl and D. J. Curran, *Anal. Chem.* **51** (1979) 353.

[20] W. J. Blaedel and J. Wang, *ibid.* **51** (1979) 799.

[21] A. N. Strohl and D. J. Curran, *ibid.* **51** (1979) 1050.

[22] W. J. Blaedel and J. Wang, *ibid.* **52** (1980) 76.

[23] *Idem, ibid.* **52** (1980) 1697.

[24] J. Wang and H. D. Dewald, *J. Electrochem. Soc.* **130** (1983) 1814.

[25] I. C. Agarwal, A. M. Rochon, H. D. Gesser and A. B. Sparling, *Water Res.* **18** (1984) 227.

[26] M. Matlosz and J. S. Newman, *J. Electrochem. Soc.* **133** (1986) 1850.

[27] A. Tentorio and U. Casolo-Ginelli, *J. Appl. Electrochem.* **8** (1978) 195.

[28] D. Cox, Ph.D. Thesis, University of Southampton, England (1982).

[29] J. M. Marracino, F. Coeuret and S. Langlois, *Electrochim. Acta* **32** (1987) 1303.

[30] S. Langlois and F. Coeuret, *J. Appl. Electrochem.* **19** (1989) 43.

[31] *Idem, ibid.* **19** (1989) 51.

[32] S. Langlois, J. O. Nanzer and F. Coeuret, *ibid.* **19** (1989) 736.

[33] F. C. Walsh and I. Whyte, unpublished work.

[34] I. F. MacDonald, M. S. El Sayed, K. Mow and F. A. Dullien, *Inq. Eng. Chem. Fund.* **18** (1979) 199.

[35] C. W. Crawford and O. A. Plumb, *J. Fluids Eng.* **108** (1986) 343.

[36] 'The Handbook of Physics and Chemistry', The Chemical Rubber Company.

[37] R. Greef, R. M. Peat, L. M. Peter, D. Pletcher and J. Robinson, 'Instrumental Methods in Electrochemistry', Ellis Horwood, Chichester (1985).

[38] A. J. Arvia, J. C. Bazan and J. S. W. Carrozza, *Electrochim. Acta* **11** (1966) 881.

[39] A. R. Gordon and A. Cole, *J. Phys. Chem.* **40** (1936) 733.

[40] D. Pletcher, F. C. Walsh and I. Whyte, *J. Cleaner Technol.*, in preparation.

[41] F. Lapique, J. M. Hornut, A. Louchkoff and A. Storck, *J. Appl. Electrochem.* **19** (1989) 195.